



저작자표시-비영리-동일조건변경허락 2.0 대한민국

이용자는 아래의 조건을 따르는 경우에 한하여 자유롭게

- 이 저작물을 복제, 배포, 전송, 전시, 공연 및 방송할 수 있습니다.
- 이차적 저작물을 작성할 수 있습니다.

다음과 같은 조건을 따라야 합니다:



저작자표시. 귀하는 원저작자를 표시하여야 합니다.



비영리. 귀하는 이 저작물을 영리 목적으로 이용할 수 없습니다.



동일조건변경허락. 귀하가 이 저작물을 개작, 변형 또는 가공했을 경우에는, 이 저작물과 동일한 이용허락조건하에서만 배포할 수 있습니다.

- 귀하는, 이 저작물의 재이용이나 배포의 경우, 이 저작물에 적용된 이용허락조건을 명확하게 나타내어야 합니다.
- 저작권자로부터 별도의 허가를 받으면 이러한 조건들은 적용되지 않습니다.

저작권법에 따른 이용자의 권리는 위의 내용에 의하여 영향을 받지 않습니다.

이것은 [이용허락규약\(Legal Code\)](#)을 이해하기 쉽게 요약한 것입니다.

[Disclaimer](#)

도시계획학 석사학위논문

**The Net Flux of CO₂ Evasion from a
Stream in a Small Forested Watershed
under Monsoon Climates**

계절풍 기후대의 산림 소유역 하천에서 대기로
이동하는 이산화탄소의 양

2015 년 2월

서울대학교 환경대학원

환경계획학과 환경관리전공

고은별

The Net Flux of CO₂ Evasion from a Stream in a Small Forested Watershed under Monsoon Climates

지도교수 오능환

이 논문을 도시계획학 석사학위논문으로 제출함

2014년 2월

서울대학교 환경대학원
환경계획학과 환경관리전공
고은별

고은별의 석사학위논문을 인준함

2015년 2월

위원장 이 동 수 (인)

부위원장 박 지 형 (인)

위 원 오 능 환 (인)

Abstract

**The Net Flux of CO₂ Evasion from a
Stream in a Small Forested Watershed
under Monsoon Climates**

Ko, Eun Byul

Environmental Planning, Environmental Management

The Graduate School of Environmental Studies

Seoul National University

The amount of CO₂ that evades from streams to the atmosphere particularly in headwater regions is an important piece of the regional and global carbon cycle. Although CO₂ evasion from inland waters can be larger than riverine export of carbon, stream-specific data on CO₂ evasion are still rare, especially in regions under Asian monsoon climates. I investigated stream pCO₂ dynamics in Bukmoon-gol forested watershed of Mt. Baekwoon in Junlanam-do, Republic of Korea (South Korea) spanning the period May 2012-April 2014 to quantify annual net flux of CO₂ evasion using stream water samples collected weekly as well as every 2-4 hours during summer storms. The specific objectives of this study are to quantify the annual flux of CO₂ evasion from a forest stream and compare it to the

annual lateral DIC export; and to identify the factors influencing stream CO₂ evasion. Stream water pCO₂ was calculated based on the carbonate equilibria with pH, water temperature, and alkalinity measurements. Gas transfer velocities were estimated using three different empirical models. The annual mean CO₂ evasion flux per unit area of the watershed was estimated to be in the range of 0.06 to 0.12 g C m⁻² yr⁻¹ which was about up to 12% of the annual lateral DIC flux over the same period. During the summer monsoon periods, high discharge can increase the gas transfer velocity due to increased stream velocity, elevating net CO₂ evasion from the stream. The gas transfer velocities from the three different model equations ranged from 2.3 to 115 m d⁻¹, resulting in large variation in weekly stream CO₂ evasion. The results suggest that net CO₂ evasion in a temperate forest stream under monsoon climates can be a significant component of regional carbon cycle despite the low proportion of stream area in a watershed.

keywords : CO₂ evasion, forest, Monsoon, pCO₂, stream, watershed

Student Number : 2012-23783

Table of Contents

I. Introduction	1
II. Materials and Methods	7
1. Study site.....	7
2. pCO ₂ gradient and water chemistry	8
3. Stream-air CO ₂ flux.....	11
3.1. The two-film model.....	11
3.2. The net flux of CO ₂ at air-water interface.....	12
4. Gas transfer velocity models for streams	13
5. Annual CO ₂ evasion flux for the watershed	15
III. Results and Discussion	16
1. pCO ₂ variation in forest streams	16
1.1. Streams as a potential source of CO ₂	16
1.2. Temporal variation of pCO ₂ in stream water	16
1.3. Spatial variation of pCO ₂ in stream water	21
1.4. The effect of monsoon on pCO ₂ variation.....	21
2. Models for gas transfer velocities.....	28
3. Annual CO ₂ evasion flux of the forest stream	29
IV. Implications and limitations	33
References	36
국문초록	42

List of Figures

Figure 1. The study site in Bukmoon-gol and Baram-gol experimental watersheds on a 1:25,000-scale digital elevation model (DEM). The mouth of the Baram-gol watershed is indicated as “B1”, the mouth of the first-order stream of Bukmoon-gol watershed as “A2,” and the mouth of the second-order stream of Bukmoon-gol watershed as “A1” where hourly discharge was measured. This figure is created by Ms. Eun-Ju Lee at Seoul National University (unpublished data).	8
Figure 2. A graphical representation of the simple two-film model for the air-water exchange of CO ₂ gas. C _g and C _w represent concentrations of CO ₂ gas in air and in water respectively. C _g [*] and C _w [*] represent concentration of CO ₂ gas in the stagnant layer in air and in water respectively (Whitman, 1923).	11
Figure 3. Water temperature, stream discharge, and weekly pCO ₂ from May 2012 to April 2014 at A1. The black dot is pCO ₂ of the stream water (µatm) equilibrated with air; the blue dashed line is the water temperature (°C) estimated from the air temperature (°C); and the red line is average daily discharge (m ³ s ⁻¹). (a) with all weekly pCO ₂ data, and (b) without the 7 largest pCO ₂ data points (> 4,000 µatm).....	17
Figure 4. (a) Relationship between weekly stream pCO ₂ and average daily discharge; (b) relationship between weekly stream pCO ₂ and estimated water temperature; (c) relationship between weekly stream pCO ₂ and average daily discharge without the 7 largest pCO ₂ data points (> 4,000 µatm); and (d) relationship between weekly stream pCO ₂ and estimated water temperature without the 7 largest pCO ₂ data points (> 4,000 µatm).....	18
Figure 5. Weekly stream water pCO ₂ (µatm) at A1 and A2 from May 2012 to April 2014, calculated by the CO2SYS program. The black triangles indicate pCO ₂ at A2 and the red circles at A1. The high amount of pCO ₂ in winter of 2014 was due to low pH which could overestimate water pCO ₂	21
Figure 6. Calculated stream pCO ₂ , estimated hourly discharge, and hourly rainfall during storm events in (a) 2012 and (b) 2013. Black bars indicate hourly rainfall (mm); red dotted line indicates discharge (m ³ s ⁻¹); and black dotted line represents stream pCO ₂ (µatm).	23
Figure 7. (a) Calculated pCO ₂ in µatm (red dotted line) and hourly rainfall in mm (black bars) at A1; and (b) calculated pCO ₂ in µatm (red dotted line), average hourly water temperature in °C (brown triangles), average hourly DO concentration in mg L ⁻¹ (blue line), hourly rainfall in mm (black bars), and average hourly pH (black dotted line) during the typhoon NAKRI.	26

Figure 8. a) Cl⁻ and SO₄²⁻ concentrations (mg L⁻¹) at A1 during typhoon NAKRI. b) NO₃-N (mg L⁻¹) and DOC (mg L⁻¹) concentrations at A1 during the typhoon NAKRI.27

Figure 9. Temporal variation of k_{CO2} depending on three different models at A1. k_{CO2} are in units of m d⁻¹. The red dots, the green dots, and the black dots are results of model 1, 2, and 3, respectively.28

List of Tables

Table 1. Three gas transfer velocity models for streams. V = stream velocity (m s⁻¹); S = stream slope (unitless); D = stream depth (m); and Q = stream discharge (m³ s⁻¹).14

Table 2. Empirical equations used to estimate width and depth of the stream. Discharge was measured at the weir (m³ s⁻¹). Units: width (m), depth (m), and discharge (m³ s⁻¹).15

Table 3. Average values of calculated pCO₂, pH, Alkalinity (Alk.), and DOC at different ranges of pH at A1. Average values of measured pCO₂, pH, Alk., and DOC in other countries were also listed.20

Table 4. Mean fluxes calculated with three gas transfer velocity models that utilize physical characteristics of the stream and hydrology. Median k_{CO2} are in bold and minimum and maximum k_{CO2} are in parenthesis. Mean fluxes are presented with standard deviation in parenthesis.31

Table 5. Summary of precedent research for evasion of CO₂ from streams (modified from the Table 4 by Wallin *et al.* (2012)).32

I. Introduction

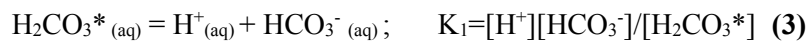
Carbon dioxide (CO₂) is one of the most important anthropogenic greenhouse gases that contributes to climate change (IPCC, 2007). Since the Industrial Revolution, the concentration of CO₂ in the atmosphere has continuously increased from about 280 parts per million by volume (ppmv) to above 400 ppmv in 2013 (NOAA, 2013). Rising anthropogenic CO₂ emissions from fossil fuels and land-use change have perturbed the natural global carbon cycle that controls climate system (IPCC, 2007). According to the global carbon budget in 2013, anthropogenic sources and land-use change emitted 10.8 ± 0.5 Pg C yr⁻¹ to the atmosphere; the ocean and terrestrial ecosystem sequestered 2.9 ± 0.5 Pg C yr⁻¹ and 2.5 ± 0.5 Pg C yr⁻¹ respectively; and the rest remained in the atmosphere (The Global Carbon Project, www.globalcarbonproject.org).

The traditional global carbon cycle model considered inland waters as just a passive aquatic conduit that simply delivers carbon from land to ocean (Siegenthaler and Sarmiento, 1993). However, a revised model suggested that inland waters can be considered as a “tapered pipe” where loss of carbon occurs during the transport to the ocean via sedimentation and CO₂ outgassing to the atmosphere (Cole *et al.*, 2007). Many studies have demonstrated that inland waters such as lakes, rivers, reservoirs, and streams are supersaturated with CO₂ with respect to the atmosphere acting as CO₂ sources (Cole *et al.*, 2007; Aufdenkampe *et al.*, 2011; Butman and Raymond, 2011; Raymond *et al.*, 2012; Li and Zhang, 2014). Global CO₂ outgassing estimates for inland waters were estimated to be 1.8

Pg C yr⁻¹ from streams and rivers, and 0.32 Pg C yr⁻¹ from lakes and reservoirs (Raymond *et al.*, 2013).

The exchange of CO₂ across the water-air interface is driven by chemical potential differences of CO₂ across the water-air interfaces and the gas exchange ability that is expressed as gas transfer velocity (Cole *et al.*, 1998; Raymond *et al.*, 2012). The chemical potential differences of CO₂ at the water-air interface determine the direction and magnitude of the flux either positive or negative (Cole *et al.*, 1998). The positive, upward flux of CO₂ from water surface to the air is known as evasion of CO₂, whereas the negative flux of CO₂ from the air to the water surface is called invasion of CO₂ (Raymond *et al.*, 2000; Raymond *et al.*, 2013).

The carbonate system in freshwaters can be described with a set of species at equilibria (equation 1, 2, 3, 4) (Stumm and Morgan, 1996):



where the equilibrium constants K_0 , K_1 , and K_2 are expressed as mol L⁻¹ atm⁻¹; $[\text{H}_2\text{CO}_3^*]$, $[\text{HCO}_3^-]$, $[\text{CO}_3^{2-}]$, and $[\text{H}^+]$ are in mol L⁻¹; and $[\text{CO}_2(\text{g})]$ is CO₂ partial pressure in air in atm.

The sum of dissolved CO₂ (CO_{2(aq)}) and pure H₂CO_{3(aq)} is conventionally

presented as H_2CO_3^* (Stumm and Morgan, 1996). Thus, H_2CO_3^* , bicarbonate (HCO_3^-), and carbonate (CO_3^{2-}) are species that represent total dissolved inorganic carbon (DIC). $\text{pCO}_{2(\text{g})}$ in equilibrium with $\text{CO}_{2(\text{w})}$ can be calculated indirectly from water chemistry parameters if any two of the following variables (pH, alkalinity, and DIC) are measured along with water temperature (Millero, 2000). pCO_2 values are often calculated using programs such as PHREEQC and CO2SYS (Hunt et al., 2011), or can be directly measured by headspace equilibration, followed by analysis of the headspace using non-dispersive infrared CO_2 analyzers or gas chromatography (Raymond et al., 1997; Raymond *et al.*, 2000; Davidson et al., 2010).

Dissolved CO_2 concentrations in water are affected by the aforementioned water chemistry parameters (pH, alkalinity, and DIC concentration). These parameters are in turn correlated with catchment properties such as carbonate proportion in soils and rocks (Lauerwald *et al.*, 2013). CO_2 in soils via plant-root and microbial respiration and groundwater input throughout hydrologic pathways can drive the stream dissolved CO_2 concentration (Pinol and Avila, 1992; Jones and Mulholland, 1998; Finlay, 2003). With increasing canopy covers, dissolved CO_2 concentration can increase during summer at base flows (Finlay, 2003). Other factors that can affect dissolved CO_2 concentration in streams are in-stream processes (photosynthesis and respiration) and CO_2 evasion (Wetzel, 1983; Wetzel and Likens, 1991; Hope *et al.*, 1994; Dawson *et al.*, 2001).

Gas transfer velocity in addition to pCO_2 gradient is another important

term in the flux equation that depends on parameters such as surface water turbulence and wind speed (Raymond and Cole, 2001; Alin *et al.*, 2011). Gas transfer velocity can be directly measured or indirectly estimated using empirical equations (Raymond *et al.*, 2013). Gas transfer velocities should be chosen depending on types of surface waters. For instance, gas transfer velocity for streams is dependent on water turbulence that is influenced by discharge and physical characteristics of streams such as slope, width, and depth (Wallin *et al.*, 2011; Raymond *et al.*, 2012).

The CO₂ evasion is greater in headwater streams compared to rivers downstream due to higher water turbulence (Raymond *et al.*, 2013). Stream pCO₂ is dependent on stream order such that stream pCO₂ decreased as stream discharge increased suggesting that headwater streams are hotspots of CO₂ evasion (Teodoru *et al.*, 2009; Dinsmore *et al.*, 2011; Crawford *et al.*, 2013). More than 90% of CO₂ can escape to the atmosphere from streams within headwater reaches (Johnson *et al.*, 2008). Stream CO₂ evasion from streams can be greater in magnitude than the lateral downstream export of carbon in the form of dissolved organic carbon (DOC) and dissolved inorganic carbon (DIC) according to a study conducted in a boreal forested catchment in Northern Sweden; CO₂ evasion may account for 53 % of the combined lateral and vertical carbon export from the stream per catchment area (Wallin *et al.*, 2013). Lack of stream-specific data such as length, width, and stream surface area and high spatiotemporal variability of CO₂ concentrations in stream and gas transfer velocities have made it difficult to correctly estimate the net flux of CO₂ evasion from inland waters both at regional and global scale (Cole

et al., 1998; Cole *et al.*, 2007; Wallin *et al.*, 2011; Dinsmore *et al.*, 2013; Lauerwald *et al.*, 2013).

During summer, Asian monsoon drastically affects stream and river carbon dynamics in South Korea as well as other East Asian countries with more than 50% of the annual precipitation (1,000~1,800 mm) and rapid overland flow (Kim *et al.*, 2007; Korea Meteorological Administration, www.kma.go.kr). Although several studies have reported the lateral flux of stream carbon in forested watersheds in South Korea during East Asian monsoon (Kim *et al.*, 2007; Kim *et al.*, 2010; Jeong *et al.*, 2012), none has examined stream pCO₂ evasion in forested watersheds in South Korea except one study. The flux of CO₂ evasion from headwater regions in South Korea had been calculated based on biweekly stream water sampling at base flow, however it may not be enough to understand pCO₂ dynamics in changing water regime during East Asian monsoon (Shin *et al.*, 2011). Considering that 64% of area of South Korea is covered by forests, understanding what controls pCO₂ dynamics and quantifying the net flux of stream CO₂ evasion from a forested headwater stream can serve as an milestone in providing a baseline for future studies, not only applicable to national studies, but also for related research in other Asian countries under monsoon climates.

The specific objectives of this study are to quantify the annual flux of CO₂ evasion from a forest stream (May 2012-April 2014) and investigate the factors influencing stream CO₂ evasion. I investigated stream pCO₂ dynamics in Bukmoon-gol forested watershed of Mt. Baekwoon in South Korea spanning the

period May 2012-April 2014 to quantify annual flux of CO₂ evasion using stream water samples collected weekly as well as at every 2-4 hrs during storms.

II. Materials and Methods

1. Study site

The first- and second-order streams are located within the Bukmoon-gol forested watershed in Mt. Baekwoon, Gyang-si, South Korea (35.0319° N, 127.6050° E) (Figure 1). The size of the watershed is 33.3 ha (or 0.333 km²) (Woo, 2000). The stream slope and the main stream length of the entire Bukmoon-gol watershed derived from a digital map (1:5,000 scale) were 25.3% and 850 m, respectively (Choi, 2001).

Vegetation in the watershed consists of mixed coniferous and deciduous forests including *Pinus densiflora*, *Pinus rigida*, *Pinus taeda* and *Castanea crenata* (Im *et al.*, 2007). *Castanea crenata* accounts for about 30% of the entire watershed and the average depth of O-horizon and A-horizon is 5.9 cm and 24.1 cm, respectively (Im *et al.*, 2007). The bedrock of this region is mainly granite and partially gneiss and the soils are sandy loam, and clay loam (Park *et al.*, 2000). According to geological data, the catchment is dominated by Pre-cambrian porphyroblastic gneiss (Korea Institute of Geoscience and Mineral Resources, <http://geoinfo.kigam.re.kr>).

Hourly stream discharge (m³ s⁻¹) was measured using sharp-crested rectangular weirs (Combalicer *et al.*, 2008). The depth of overflowing stream water at the outlet and the observed stream water depth were converted into discharge using water depth-discharge curve (Combalicer *et al.*, 2008). Unfortunately, the

discharge data were not recorded between May and August in 2014 due to malfunction of the equipment.

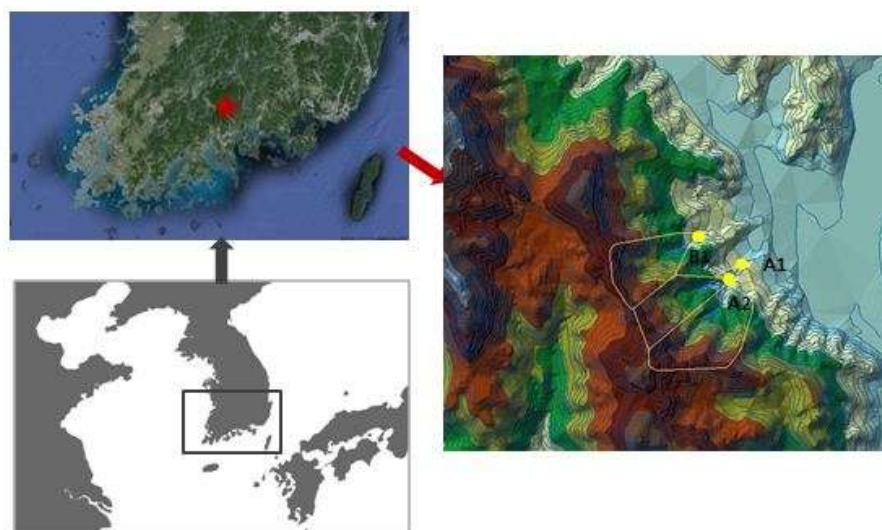


Figure 1. The study site in Bukmoon-gol and Baram-gol experimental watersheds on a 1:25,000-scale digital elevation model (DEM). The mouth of the Baram-gol watershed is indicated as “B1”, the mouth of the first-order stream of Bukmoon-gol watershed as “A2,” and the mouth of the second-order stream of Bukmoon-gol watershed as “A1” where hourly discharge was measured. This figure is created by Ms. Eun-Ju Lee at Seoul National University (unpublished data).

2. pCO₂ gradient and water chemistry

Stream water samples have been collected in a ponding basin of a U-shaped weir every week since December in 2011. Sampling time was kept consistent at 10 a.m. because photosynthesis and respiration could fluctuate during the day (Halbedel and Koschorreck, 2013). Storm water samples were collected manually using 1 L polycarbonate or polyethylene bottles during the four campaigns (June 29th - July 1st, 2012; July 5th - June 15th, 2012; July 3rd - July 8th, 2013; and August 2nd - August 5th, 2014) at 2 to 4 hour intervals. Water samples

were transported to the lab on ice and filtered through pre-combusted glass fiber filter (pore size of 0.7 μm). Water pH (Metrohm AG., Switzerland), electrical conductivity (YSI Inc., USA), and alkalinity were measured the next day and then samples were kept frozen until other analysis including major ion and DOC concentrations. A total of 20 water samples were analyzed for water pH after >two days of sampling and these data were excluded from the analysis. Water pH was also measured in the field (YSI Inc., USA) for the storm samples. Both pH meters were calibrated against pH 4.0 and 7.0 calibration solutions (YSI Inc., USA) prior to analysis. DOC concentration was measured by a Shimadzu TOC-5500 (Shimadzu Corporation, Japan). Concentrations of major anions (F^- , Cl^- , NO_3^- , and SO_4^{2-}), and cations (Na^+ , K^+ , NH_4^+ , Mg^{2+} , and Ca^{2+}) were analyzed by ion chromatography (IC) (Dionex, Sunnyvale, USA). The accuracy of the measurements were tested using secondary standard materials and recovery was between 90% and 100% of the certified values.

Alkalinity is defined as follows (Schlesinger and Bernhardt, 2013):

$$\text{Alkalinity} = [\text{HCO}_3^-] + 2[\text{CO}_3^{2-}] + [\text{OH}^-] - [\text{H}^+] \quad (5)$$

Thus, alkalinity can be also calculated using the charge balance equation (eq. 6) (Schlesinger and Bernhardt, 2013):

$$\text{Alkalinity} = 2*[\text{Ca}^{2+}] + 2*[\text{Mg}^{2+}] + [\text{Na}^+] + [\text{K}^+] + [\text{NH}_4^+] - 2*[\text{SO}_4^{2-}] - [\text{NO}_3^-] - [\text{Cl}^-] \quad (6)$$

Alkalinity calculated by eq. (6) was used in this study. Alkalinity along with pH measurements and water temperature data were used to calculate carbonate speciation of DIC including pCO_2 over April 2012–May 2014 using the

CO2SYS program (Lewis and Wallace, 1998).

Water temperature was monitored using a sensor (Hobo stainless temperature data logger, Onset computer Inc., USA) from March, 2014 to August, 2014 and an empirical relationship between air temperature and water temperature was used for the period when water temperature data were not available ($T_{\text{water}}=0.64*T_{\text{air}}+4.09$; $R^2=0.73$; $p\text{-value}<0.001$). This approach using the relationship between air temperature and water temperature had been incorporated to estimate $p\text{CO}_2$ at regional scale (Raymond *et al.*, 2013).

3. Stream-air CO₂ flux

3.1. The two-film model

The two-film model assumes that a stable stagnant layer having some thicknesses exists in water and in air in the absence of turbulence (Figure 2), and this simple model can be applied to the exchange of CO₂ between air and water (Whitman, 1923).

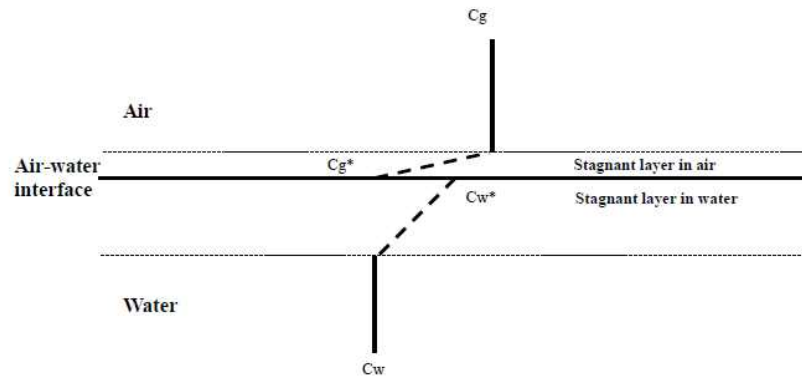


Figure 2. A graphical representation of the simple two-film model for the air-water exchange of CO₂ gas. C_g and C_w represent concentrations of CO₂ gas in air and in water respectively. C_g^* and C_w^* represent concentration of CO₂ gas in the stagnant layer in air and in water respectively (Whitman, 1923).

Applying Fick's first law, the flux of CO₂ through the stagnant layers can be calculated as follows (Liss and Slater, 1974):

$$F = k \times \Delta C \quad (7)$$

$$F = k_g \times (C_g - C_g^*) = k_w \times (C_w^* - C_w) \quad (8)$$

where, F is the flux of gas; k is the exchange constant; ΔC is the concentration gradient across the different phases; k_g is the exchange constant in the gas phase; C_g is the concentration in the gas phase; C_g^* is the concentration in the stagnant

layer of the gas phase; k_w is the exchange constant in the water phase; C_w is the concentration in the water phase; and C_w^* the concentration in the stagnant layer of the water phase.

The concentrations of CO_2 are always measured above or below the stagnant layers and the terms C_g^* and C_w^* can be deleted and the equation (8) can be re-written as (Sarmiento and Gruber, 2006):

$$F = K \times (C_g - C_w) \quad (9)$$

$$\text{where } 1/K = 1/k_g + 1/k_w \quad (10)$$

Since the water phase has been found to control the exchange of CO_2 at the air-water interface (Liss and Slater, 1974), the term $1/k_g$ can be ignored (Sarmiento and Gruber, 2006).

So, the equation (10) can be rearranged as follows (Sarmiento and Gruber, 2006):

$$1/K = 1/k_w \quad (11)$$

Thus, the net flux of a gas from two phases can be estimated following equation (eq. 12) (Sarmiento and Gruber, 2006):

$$F = k_w \times (C_g - C_w) \quad (12)$$

3.2. The net flux of CO_2 at air-water interface

Estimating evasion of CO_2 uses interfacial mass transfer equations (Borges *et al.*, 2004). The first step is to estimate partial pressure differences between air and stream water equilibrated with the air. The second step is to estimate the gas transfer velocity (Cole *et al.*, 1998) and only water-side gas transfer

velocity is considered for the CO₂ exchange at air-water interface (eq. 11). Finally, combining knowledge about pCO₂ and gas transfer velocity will allow one to estimate the amount of vertical export of CO₂ (eq. 15) (Cole *et al.*, 1998; Zappa *et al.*, 2003; Maria de Fátima *et al.*, 2013; Li and Zhang, 2014):

$$F_{\text{CO}_2} = k * K_h * (p\text{CO}_{2\text{eq}} - p\text{CO}_{2\text{air}}) \quad (13)$$

where F_{CO_2} is the diffusive net flux of CO₂ ($\mu\text{mol m}^{-2} \text{d}^{-1}$), k is gas transfer velocity (m d^{-1}), K_h is the temperature-dependent Henry's constant ($\text{mol L}^{-1} \text{atm}^{-1}$ ($=10^3 \text{ mol m}^{-3} \text{atm}^{-1}$)), $p\text{CO}_{2\text{eq}}$ is equilibrated partial pressure of CO₂ (aq) in μatm , and $p\text{CO}_{2\text{air}}$ is $p\text{CO}_2$ in air in μatm . K_h was estimated using the following equation (Weiss, 1974):

$$\ln K_h = A + B(100/T) + C * \ln(T/100) \quad (14)$$

where T is temperature in Kelvin, and A , B , and C are the constants, -58.0931, 90.5069, and 22.2940, respectively.

4. Gas transfer velocity models for streams

In order to estimate the gas transfer velocity for streams, empirical equations in the literature that have incorporated stream water turbulence were used. The following three empirical equations suitable for small streams were used (Table 1).

Table 1. Three gas transfer velocity models for streams. V = stream velocity (m s⁻¹); S = stream slope (unitless); D = stream depth (m); and Q = stream discharge (m³ s⁻¹).

No.	Model	Reference
1	$k_{600}=(VS)^{0.89}*D^{0.54}*5037$ ($r^2 = 0.72$)	(Raymond <i>et al.</i> , 2012)
2	$k_{600}=VS*2841+ 2.02$ ($r^2 = 0.55$)	(Raymond <i>et al.</i> , 2012)
3	$k_{600}=4725*(VS)^{0.86}*Q^{-0.14}*D^{0.66}$ ($r^2 = 0.76$)	(Raymond <i>et al.</i> , 2012)

In the Table 1, the model 1, 2, and 3 refers to as gas transfer velocity models for streams and rivers expressed in the form of k_{600} . The k_{600} is known as the Schmidt number of 600 which is the ratio of the kinematic viscosity of water to the diffusion coefficient normalized to CO₂ at 20 °C (Raymond *et al.*, 2012). k_{600} is a commonly reported values in the literature (Raymond *et al.*, 2012). Using the equation (16) and (17), k_{600} can be converted into the actual gas transfer velocity (k_{CO_2}) (Wanninkhof, 1992):

$$k_{CO_2} = k_{600}*(Sc_T/600)^{-0.5} \quad (15)$$

where k_{CO_2} is the actual gas transfeser velocity to be used (m d⁻¹);

k_{600} (m d⁻¹); and Sc_T is the Schmidt number for CO₂ in the equation (eq. 16).

$$Sc_T = 1742-91.24*T+2.208*T^2-0.0219*T^3 \quad (16)$$

where Sc_T is the Schmidt number for CO₂ for 4-35 °C; and T is the water temperature in °C.

5. Annual CO₂ evasion flux for the watershed

The main stream length for the Bukmoon-gol watershed was estimated to be 850 m for the entire watershed using 30 m x 30 m resolution DEM which was similar to the previously reported value (Choi, 2001). The stream width and depth were estimated using empirical hydraulic geometry relationships with discharge (Raymond *et al.*, 2012). The stream velocity was estimated by dividing water discharge with cross-sectional area.

Table 2. Empirical equations used to estimate width and depth of the stream. Discharge was measured at the weir (m³ s⁻¹). Units: width (m), depth (m), and discharge (m³ s⁻¹).

	Equations used	References
Width	$\ln(\text{width}) = 2.56 + \ln(\text{discharge}) * 0.423$ ($r^2 = 0.82$)	(Raymond et al., 2012)
Depth	$\ln(\text{depth}) = -0.895 + \ln(\text{discharge}) * 0.294$ ($r^2 = 0.62$)	(Raymond et al., 2012)

Weekly CO₂ evasion was estimated and then the average values were converted to mean annual net CO₂ evasion from the stream. The calculated flux was divided by the entire watershed area corresponding to A1 (= 0.33 km² = 330,000 m²) in Figure 1 to estimate the net CO₂ evasion from the watershed.

III. Results and Discussion

1. pCO₂ variation in forest streams

1.1. Streams as a potential source of CO₂

Calculated stream water pCO₂ in the first-order stream (A2 in Figure 1) in Bukmoon-gol watershed ranged from 92.8 to 10,762 μatm with a mean pCO₂ of 1,458.6 (SD: ±1,670.4) μatm from May 2012 to April 2014. A total of 76 stream water samples (=90.6 %) out of 83 samples showed that the stream was supersaturated in relation to atmospheric CO₂ concentration of 400 ppmv. In case of the second-order stream in Bukmoon-gol watershed (A1 in Figure 1), calculated stream water pCO₂ ranged from 178.8 to 12,841.6 μatm with a mean of 1,533.8 (SD: ±2040.3) μatm during the two years. A total of 75 stream water samples (=83.9 %) out of 84 samples showed that the stream was supersaturated in relation to atmospheric CO₂ concentration of 400 ppmv. Therefore, both the first-order and second-order streams in the watershed can act as potential sources of CO₂ to atmosphere.

1.2. Temporal variation of pCO₂ in stream water

Temporal fluctuations of stream pCO₂ were observed throughout the sampling period at A1 in Bukmoon-gol watershed (Figure 3). Stream pCO₂ decreased as water discharge increased suggesting dilution effects (Figure 4) while the effects of temperature on stream pCO₂ was not significant at A1 ($r^2 = 0.07$, p-value= 0.01).

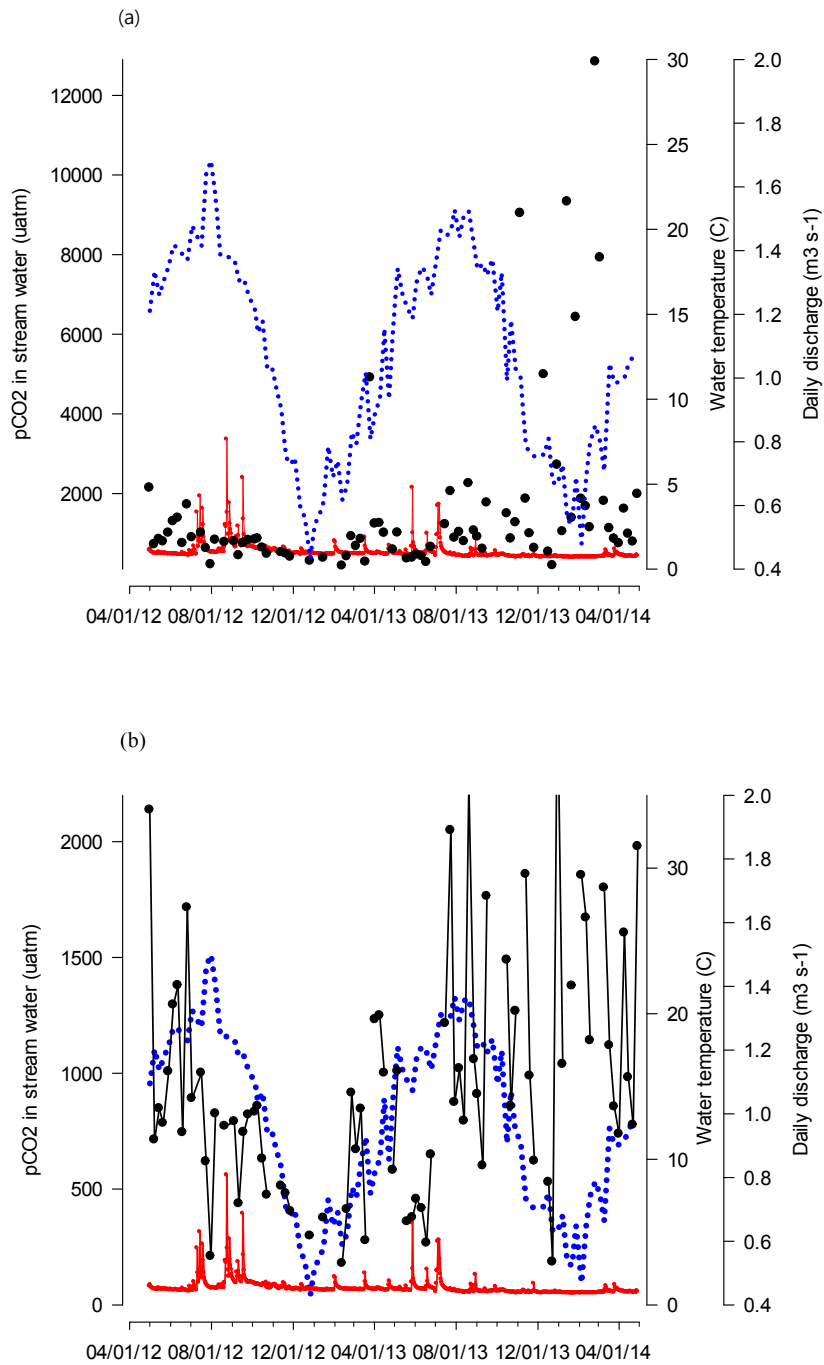


Figure 3. Water temperature, stream discharge, and weekly pCO₂ from May 2012 to April 2014 at A1. The black dot is pCO₂ of the stream water (µatm) equilibrated with air; the blue dashed line is the water temperature (°C) estimated from the air temperature (°C); and the red line is average daily discharge (m³ s⁻¹). (a) with all

weekly pCO₂ data, and (b) without the 7 largest pCO₂ data points (> 4,000 μatm).

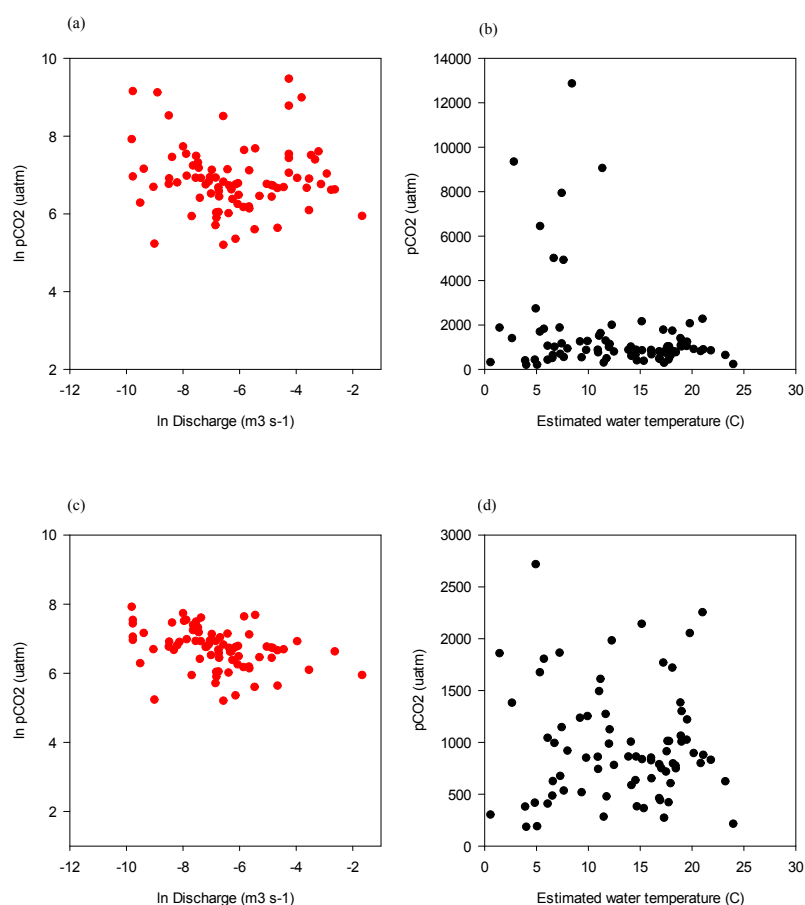


Figure 4. (a) Relationship between weekly stream pCO₂ and average daily discharge; (b) relationship between weekly stream pCO₂ and estimated water temperature; (c) relationship between weekly stream pCO₂ and average daily discharge without the 7 largest pCO₂ data points (> 4,000 μatm); and (d) relationship between weekly stream pCO₂ and estimated water temperature without the 7 largest pCO₂ data points (> 4,000 μatm).

The amplitudes of pCO₂ increased suddenly between December 2013 and April 2014 (Figure 3) due to low pH, ranging from 5.98 to 6.39 compared to the two-year mean pH of 7.1. Water pCO₂ can be significantly overestimated even with a small change of pH as pH decreases. Possible sources to these high pCO₂ values could be variation in the accuracy of the electrode based pH measurements

(Raymond *et al.*, 1997) or acidified water samples due to contribution of CO₂-rich soil water or groundwater. The accuracy of pH measurements using electrodes can be insufficient (up to 0.6 units of pH) especially for waters with a low conductivity (less than 100 $\mu\text{S cm}^{-1}$) (Neal and Thomas, 1985; Busenberg and Plummer, 1987). When alkalinity is 0.215 meq L⁻¹ (two-year average of alkalinity at A1) and water temperature is 25 °C, changing 0.6 units of pH from pH 7.0 to pH 6.4 can increase pCO₂ by 299 % (From 1,415.3 μatm to 5,648.2 μatm). The temperature difference between the calibration solutions and water samples can cause pH errors of up to 0.7 units (Neal and Thomas, 1985). However, high pCO₂ during winter in Figure 3 may not be due to the temperature difference between water samples and the calibration solutions because they were all measured in the lab at room temperature.

Averaged pCO₂, pH, alkalinity, and DOC concentrations were compared at different levels of pH (Table 3). At A1 in Bukmoon-gol watershed, the stream was characterized by very low DOC values, low alkalinity, and neutral pH for the most of the time (Table 3). Our DOC values are very low when compared to other freshwater systems in different regions of the world with similar alkalinity values (Table 3).

Stream pH readings can be unstable in low ionic-strength waters (Frankignoulle and Borges, 2001). Although the presence of organic acids can contribute to the overestimation of pCO₂ (Abril *et al.*, 2015), the DOC concentrations ranged from 0 to 2.5 mg L⁻¹, suggesting that this is unlikely.

Calculated pCO₂ was in a good agreement with measured pCO₂ under high alkalinity (2.5-4.8 meq L⁻¹) and high pH (>7.4) conditions (Frankignoulle and Borges, 2001). On the other hand, under low alkalinity (about 0.2 meq L⁻¹) and low pH (about 5) conditions, calculated pCO₂ was largely overestimated compared to measured pCO₂ (Abril *et al.*, 2005; Abril *et al.*, 2006). Recently, it has been reported that calculated pCO₂ can lead to large overestimation, particularly organic-rich, acidic, and low alkalinity freshwaters (Abril *et al.*, 2015). Therefore, in our study site, with relatively constant low alkalinity and DOC values, low pH can cause the overestimation of calculated pCO₂.

Table 3. Average values of calculated pCO₂, pH, Alkalinity (Alk.), and DOC at different ranges of pH at A1. Average values of measured pCO₂, pH, Alk., and DOC in other countries were also listed.

pH	N	N (%)	pCO ₂ (µatm)	pH	Alk. (µmolL ⁻¹)	DOC (µmolL ⁻¹)	Location (Reference)	Note
<6	1	1%	12841.6	5.98	193.03	27.78	Junlanam-do, Republic of Korea (This study)	Neutral pH, very low DOC
6-7	24	29%	3025.2	6.7	213.2	34.6		
>7	58	70%	726.3	7.3	216.5	42.0		
Total	83	100%	1537.0	7.1	215.3	39.7		
	36		1701	6.84	233	138	Rianila and Betsiboka, Madagascar (Abril <i>et al.</i> , 2015)	Intermediate pH and DOC
	97		6093	6.01	212	1002	Congo, DRC (Abril <i>et al.</i> , 2015)	Low pH, very high DOC
	92		4429	6.20	280	588	Sinnamary, French Guiana (Abril <i>et al.</i> , 2015)	Low pH, high DOC

1.3. Spatial variation of pCO₂ in stream water

The mean stream water pCO₂ at A1 and A2 were not statistically different (paired t-value=0.578; p-value=0.565) (Figure 5). Measured distance and slope between A1 and A2 was about 80 m and 21.4%, respectively. Similar water pCO₂ levels at A1 and A2 suggested that strong CO₂-rich groundwater sources were not in vicinity or low soil CO₂ production in relatively shallow mountainous soils (Johnson *et al.*, 2008).

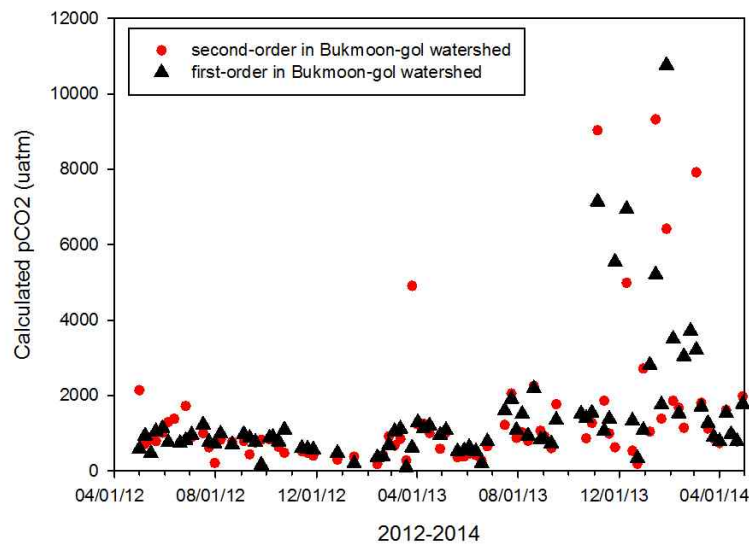


Figure 5. Weekly stream water pCO₂ (µatm) at A1 and A2 from May 2012 to April 2014, calculated by the CO2SYS program. The black triangles indicate pCO₂ at A2 and the red circles at A1. The high amount of pCO₂ in winter of 2014 was due to low pH which could overestimate water pCO₂.

1.4. The effect of monsoon on pCO₂ variation

The summer monsoon can affect stream pCO₂. Calculated pCO₂ at A1 for 2012 and 2013 storm events (Figure 6) illustrated that increased discharge (i.e. due to precipitation) brought the stream water pCO₂ levels down. This could be because

water pCO₂ was diluted by increased discharge and because water pCO₂ was outgassed by increased stream velocity and the rain drop effects that could increase gas transfer velocity (Ho *et al.*, 2007). In case of a third-order gravel stream in Austria, while stream water pCO₂ patterns showed pronounced amplitudes at base flow, these patterns were collapsed during storm events (discharge was > 3.4 m³ s⁻¹) and the patterns recovered after a few days (Peter *et al.*, 2014). Findings from this study suggested that storm events with heavy precipitation and associated increased discharge could result in a collapse in the stream pCO₂ levels (Peter *et al.*, 2014).

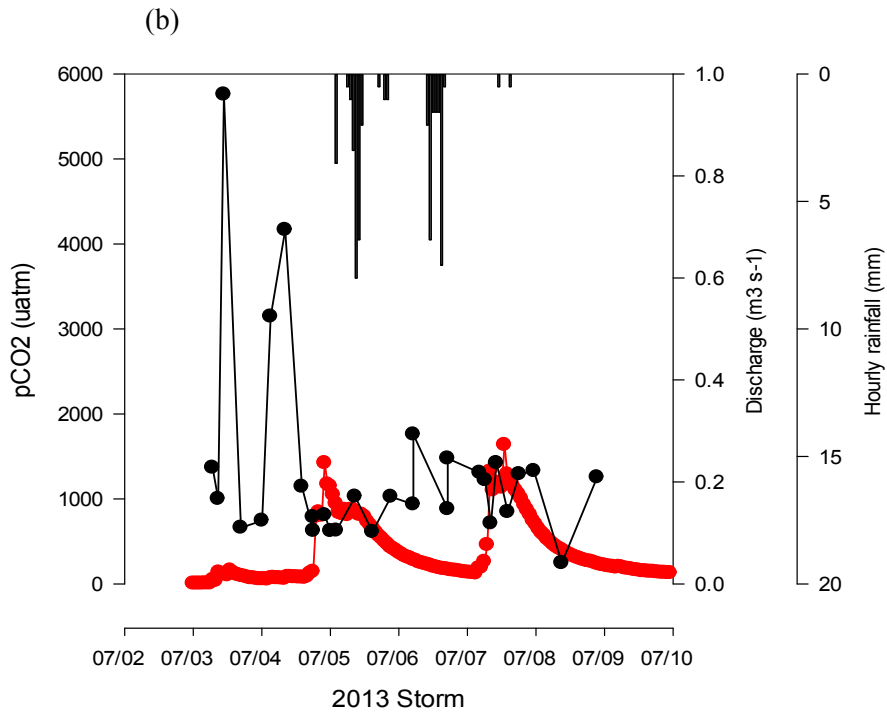
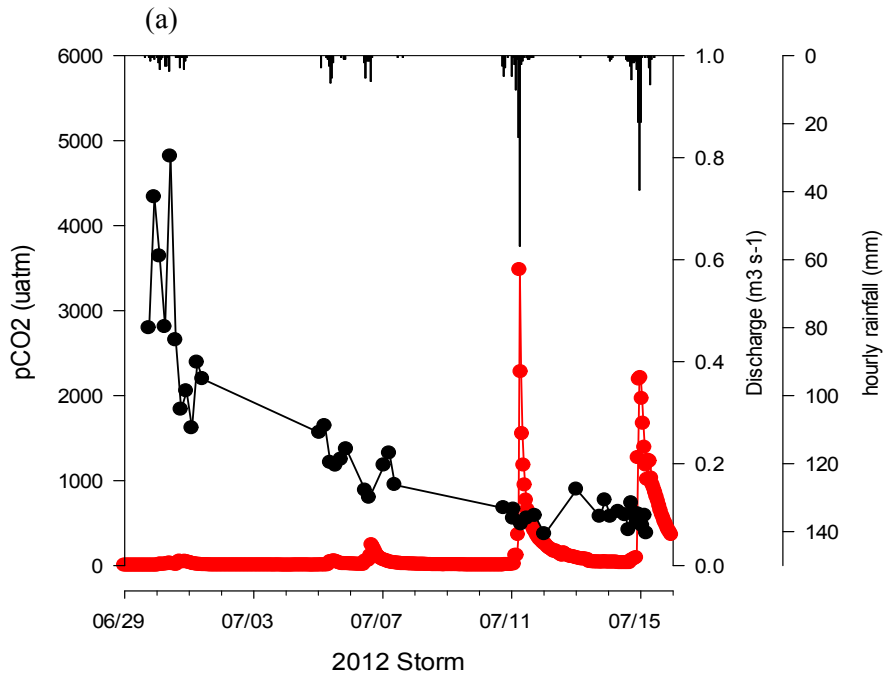


Figure 6. Calculated stream pCO₂, estimated hourly discharge, and hourly rainfall during storm events in (a) 2012 and (b) 2013. Black bars indicate hourly rainfall (mm); red dotted line indicates discharge (m³ s⁻¹); and black dotted line represents stream pCO₂ (µatm).

Three typhoons hit the Republic of Korea (the typhoon NEOGURI, HALONG, and NAKRI) from July 4 to July 11, from July 29 to August 11, from July 30 to August 3, 2014, respectively (Korea Meteorological Administration, www.typ.kma.go.kr). The monthly accumulated precipitation was recorded to be 185.7 mm in July and 716.6 mm in August, 2014. The typhoon NAKRI brought 410.6 mm of precipitation starting from the afternoon of August 2, 2014 to August 4, 2014 (Seoul National University Forest, unpublished data). During this period, calculated mean pCO₂ of the stream water at A1 was 1,377.3 (SD: ±295.7) µatm. In contrast to the storm events in 2012 and 2013, after a day of the typhoon event, stream pCO₂ changed with a smaller change of the amplitudes (Figure 7. b). The rainfall events was almost non-stop for days (Figure 7. b).

The rising pCO₂ during rainfall events may be caused by rapid transport of soil CO₂ to streams (Zeng and Masiello, 2010). NO₃⁻ and DOC concentrations in the stream water increased quickly to reach the peaks (Figure 8. b)) during the typhoon NAKRI and then dropped to the baseline concentrations after few days. In contrast, Cl⁻ and SO₄²⁻ concentrations increased and their elevated concentrations maintained even after NO₃⁻ and DOC concentrations came back to the baseline levels. The different responses of the anions during the rainfall events suggested that NO₃⁻ and DOC that originated from the forest soil quickly flushed out from the soil by the rain water and then exported to downstream due to increased stream water discharge. Thus, the forest soils could not constantly supply NO₃⁻ and DOC to the stream. Cl⁻ and SO₄²⁻ that originated from the atmospheric precipitation showed different responses because the rain acted as a constant source of these

anions. The response of the NO_3^- and DOC (Figure 8. b)) implied that soil CO_2 could not be constantly supplied to the stream during rainfall events and this was the likely reason why pCO_2 in the stream water collapsed after precipitation events and could not be recovered quickly after rain stopped.

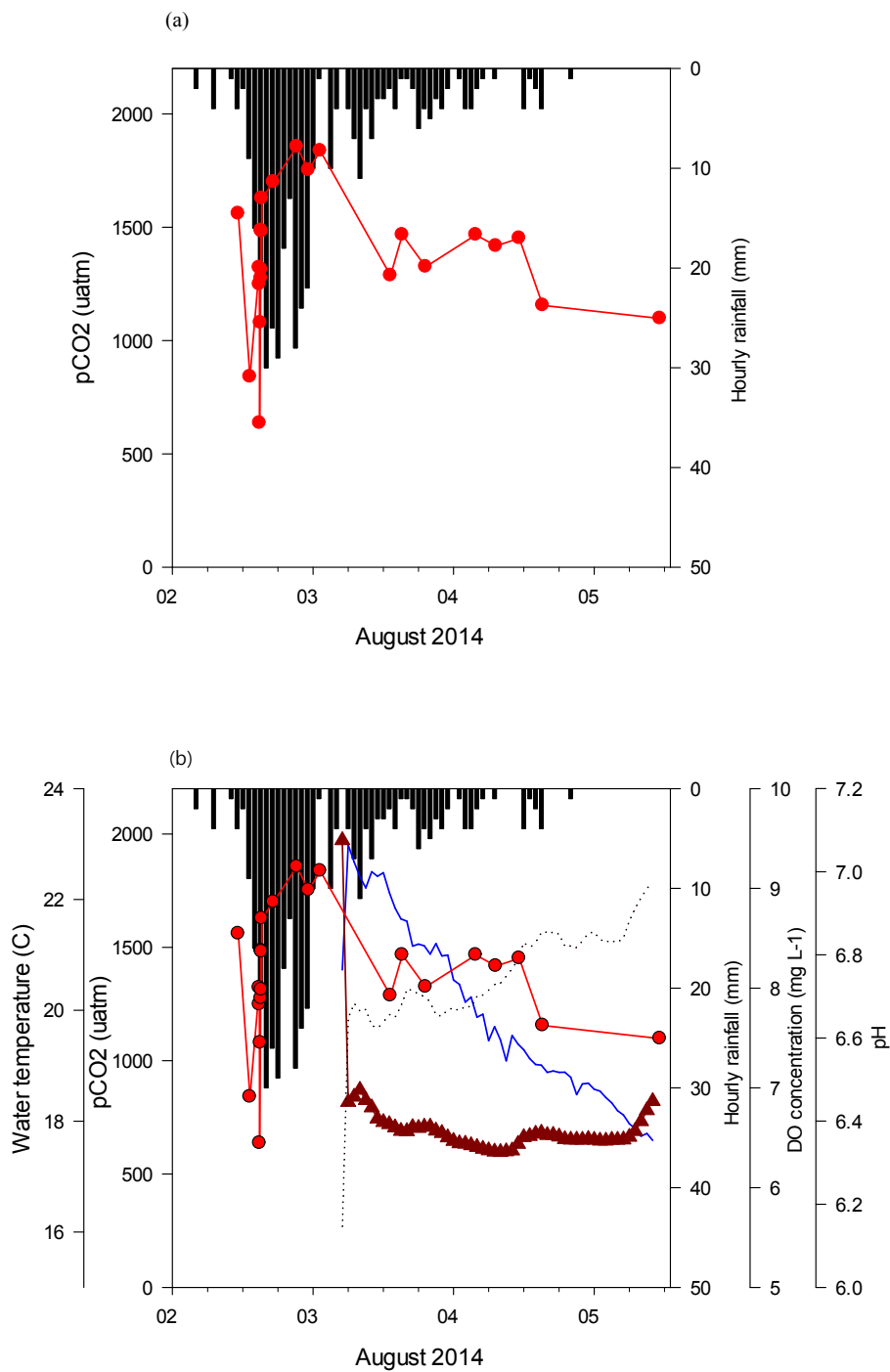


Figure 7. (a) Calculated pCO₂ in µatm (red dotted line) and hourly rainfall in mm (black bars) at A1; and (b) calculated pCO₂ in µatm (red dotted line), average hourly water temperature in °C (brown triangles), average hourly DO concentration

in mg L^{-1} (blue line), hourly rainfall in mm (black bars), and average hourly pH (black dotted line) during the typhoon NAKRI.

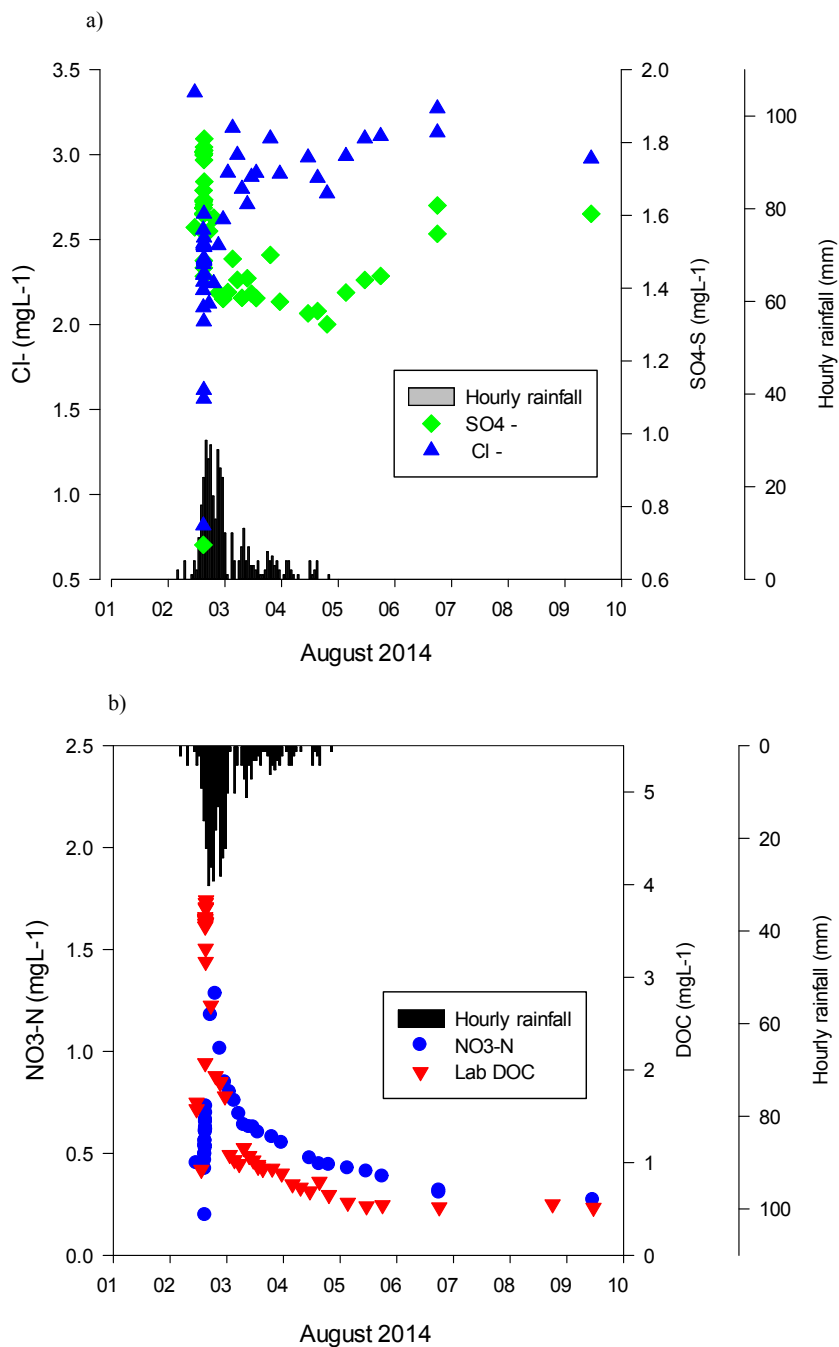


Figure 8. a) Cl^- and SO_4^{2-} concentrations (mg L^{-1}) at A1 during typhoon NAKRI. b) $\text{NO}_3\text{-N}$ (mg L^{-1}) and DOC (mg L^{-1}) concentrations at A1 during the typhoon NAKRI.

The climate (i.e. summer monsoon) and stream morphology can affect the $p\text{CO}_2$ variation in streams, resulting in temporal variations of CO_2 evasion across different seasons. These three factors are also closely linked with the ‘k’ term in the flux equation (eq. 13), controlling CO_2 evasion to the atmosphere.

2. Models for gas transfer velocities

Gas transfer velocities (k) for model 1, 2, and 3 were in the range of 2.3 – 108.5 m d^{-1} , 6.5 – 84.7 m d^{-1} , and 6.4 – 115 m d^{-1} , respectively (Figure 9). Large k values appeared during summer monsoon seasons, reflecting the potential effect of increased discharge due to precipitation inputs to the watershed. Since the term that represents mean stream slope (S) in each gas transfer velocity model equation was fixed, stream velocity (V), water depth (D), and discharge (Q) correlated to climate and hydrology were the major drivers of the temporal variation of the k values.

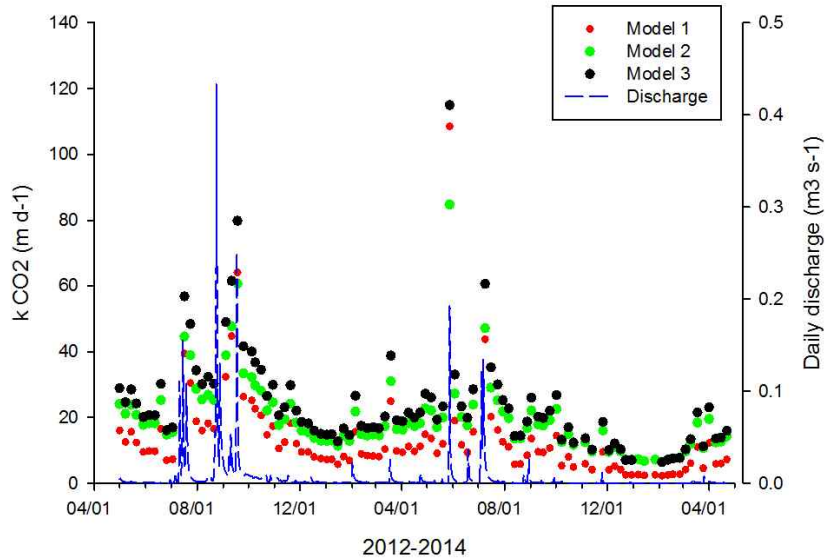


Figure 9. Temporal variation of k_{CO_2} depending on three different models at A1.

k_{CO_2} are in units of m d^{-1} . The red dots, the green dots, and the black dots are results of model 1, 2, and 3, respectively.

3. Annual CO₂ evasion flux of the forest stream

A total of 84 weekly water samples from May 2012 to April 2014 were used to estimate the annual flux of CO₂ evasion. Annual mean fluxes for stream water per the watershed based on the three gas transfer velocity model equations were from 0.06 to 0.12 g C m⁻² yr⁻¹ respectively (Table 4). Mean gas transfer velocities ranged from 13.4 to 24.1 m d⁻¹, which were greater than the average gas transfer velocities for first- and second-order streams in the U.S., 6 – 8 m d⁻¹ (Butman and Raymond, 2011) and the global average of gas transfer velocity for streams and rivers, 5.7 m d⁻¹ (Raymond *et al.*, 2013). A study that has examined the evasion flux from headwater catchments in South Korea estimated gas transfer velocities for streams ranging from 0.14 to 1.92 m d⁻¹ (Shin *et al.*, 2011) based on equation using wind speed (Waninkhof, 1992). However, the forest streams characterized by high water turbulence and mixing are different from large rivers and lakes, and the forest trees and canopies can reduce the wind speed across the forest.

Of all three model equations, model 3 that incorporated four components into the equation (stream slope, water depth, stream velocity, and discharge) may be able to provide as much information as possible to the model to explain the stream water energy dissipation and gas exchange ability between water-air interfaces. The r^2 of the model is 0.76, higher than those of the other model equations (Raymond *et al.*, 2012).

Annual lateral DIC export from this watershed during the same period was estimated to be $1.00 - 2.01 \text{ g C m}^{-2} \text{ yr}^{-1}$ (Ms. Eun-Ju Lee, unpublished data). Therefore, the vertical flux of CO_2 can be 12 % of the annual lateral DIC and 52 % of annual lateral DOC export ($0.23 - 0.43 \text{ C m}^{-2} \text{ yr}^{-1}$) (Ms. Eun-Ju Lee, unpublished data). The estimated flux of CO_2 evasion per watershed area for our study site was not high compared to other regions of the world (Table 5). Although the gas transfer velocity was high compared to its global average, the low evasion flux for the watershed suggested that the sources of the CO_2 evasion including groundwater inputs and soil CO_2 in the forest soil were limited.

Table 4. Mean fluxes calculated with three gas transfer velocity models that utilize physical characteristics of the stream and hydrology. Median k_{CO_2} are in bold and minimum and maximum k_{CO_2} are in parenthesis. Mean fluxes are presented with standard deviation in parenthesis.

k_{CO_2} model	$k_{CO_2}(m\ d^{-1})$	Mean flux per stream water ($\mu\text{mol}\ m^{-2}\ d^{-1}$)	Mean flux per stream water ($g\ C\ m^{-2}\ yr^{-1}$)	Mean flux per Bukmoon-gol watershed ($g\ C\ m^{-2}\ yr^{-1}$)
Model 1	9.7 (2.3-108.5)	8,091.4 ($\pm 12,777.5$)	35.4 (± 56)	0.06 (± 0.12)
Model 2	17.6 (6.5-84.7)	16,369.2 ($\pm 29,105.6$)	71.7 (± 127.5)	0.11 (± 0.16)
Model 3	20.3 (6.4-115)	15,868.7 ($\pm 27,748.1$)	69.5 (± 121.5)	0.12 (± 0.20)

Table 5. Summary of precedent research for evasion of CO₂ from streams (modified from the Table 4 by Wallin *et al.* (2012)).

Region	Stream order	Stream pCO ₂ (uatm)	Stream flux (g C m ⁻² yr ⁻¹)	Catchment flux (g C m ⁻² yr ⁻¹)	Remarks	References
Entire Sweden	1–6	794–1,950	473–3,032	n.a.	Stream velocity : 0.93–3.96 m s ⁻¹	(Humborg <i>et al.</i> , 2010)
Entire USA	1–10	1,588–4,326	882–4,008	4.5–22.9		(Butman and Raymond, 2011)
Gangwon-do, Republic of Korea	1–5	50.3–3,380	2–150	-0.17–0.68	DIC stream export : 12.7–38.3 g C m ⁻² yr ⁻¹	(Shin <i>et al.</i> , 2011)
Junlanam-do, Republic of Korea	1–2	179–12,842	7.51–32.2	0.06–0.12	DIC stream export : 1.0–2.01 g C m ⁻² yr ⁻¹	This study
Northern Sweden	1–5	3,400	471	0.5–2.6		(Jonsson <i>et al.</i> , 2007)
Ontario, Canada	1	3,200–9,320	311–4,347	3.1–3.9		(Billett and Moore, 2008)
Ontario, Canada	1–2	570–23,500	641–2,440	n.a.		(Koprivnjak <i>et al.</i> , 2010)
Scotland, UK	1	420–4,500	95–16,745	14.1	Peatland streams; watershed size of 130 ha; stream velocity: 0.018–0.035 m ³ s ⁻¹	(Hope <i>et al.</i> , 2001)

IV. Implications and limitations

The annual mean CO₂ evasion flux was estimated to be in the range of 0.06 to 0.12g C m⁻²yr⁻¹ which was about 12% of the annual lateral DIC flux over the same period. The factors that might have affected stream pCO₂ evasion were: (1) increased stream discharge and dilution effects due to heavy precipitation, and (2) limited supplies of soil CO₂ to the stream.

The net stream CO₂ evasion flux was the product of the partial pressure gradients between the equilibrated stream water sample and the air, the Henry's constant, and gas transfer velocity. Although each factor contributes equally to the flux estimates, the uncertainties associated with estimating gas transfer velocities seemed greater than estimating pCO₂ of stream water based on the pH, alkalinity, and water temperature data. Overestimation of the calculated pCO₂ was pronounced, particularly over the relatively low pH range. The small pH difference can result in large overestimation, particularly in waters with low alkalinity (Abril *et al.*, 2015). Indirect calculation can also underestimate pCO₂ since free CO₂ escapes to the atmosphere during filtering, pH, and alkalinity measurements (Hope *et al.*, 1995).

Many researchers have used indirect pCO₂ calculation methods to corroborate the measured values in order to minimize the uncertainties in the pCO₂ measurements. Discrete headspace samples can be analyzed for pCO₂ using CO₂ gas analyzer (Davidson *et al.*, 2010) or continuous pCO₂ measurements can be achieved using a pCO₂ equilibrator (Frankignoulle and Borges, 2001). The pCO₂

equilibrator is advantageous over discrete headspace method since time and labor can be saved. For instance, direct headspace method involves shaking the 1 L bottles to ensure that the headspace is in equilibrium with the sampled water which makes monitoring with high temporal resolution difficult (Åberg & Wallin, 2014).

Although the directly measured gas transfer velocities were not available, various empirically derived model equations for gas transfer velocities were reported. Three model equations were selected to compare gas transfer velocities among different models. While these three models produced values that were greater than reported literature values of the streams, whether or not these gas transfer velocities were representative for this watershed is remained to be tested with directly measured values in the future.

Uncertainties associated with stream surface coverage, width, and depth are also challenging. Correctly measuring the width and depth of a stream is highly complicated because they can change abruptly during rainfall. Therefore, in this study, width and depth were estimated using empirical equations and the average width and depth were 0.9 (SD:±0.9) m and 0.06 (SD:±0.04) m, respectively. The streams in the forested watershed represent dynamic environment where those stream morphological characteristics can be quickly changed upon storm and overland flooding.

The limitation of this study is that gas transfer velocity and stream-specific information including stream width and depth were estimated using U.S.A-based

empirically derived equations. A high-resolution stream $p\text{CO}_2$ data will help understand its spatiotemporal variability. Nonetheless, I provided a baseline for future studies on the flux of CO_2 evasion from streams, which could be applied to the rivers not only in South Korea, but also in other Asian countries under monsoon climates.

References

- Choi, H.-T. (2001), *Developing a rainfall-runoff model for forest watersheds using distributed hydrological concept of TOPMODEL*. Ph. D. Dissertation. Seoul National Univ.
- Combalicer, E.A. et al.(2008), “Modeling Water Balance for the Small-Forested Watershed in Korea”, 「KSCE Journal of Civil Engineering」, 12: 339-348.
- Kim, S. J. *et al.*(2007), “Hydro-Biogeochemical Approaches to Understanding of Water and Carbon Cycling in the Gwangneung Forest Catchment”, 「Korean Journal of Agricultural and Forest Meteorology」, 9(2): 109-120.
- Im, S.-J. *et al.*(2007), “Prediction of Runoff on a Small Forest Watershed Using BROOK90 Model”, 「Korean Journal of Limnology」, 40(1): 155-162.
- Park, J.-H. *et al.*(2000), “The effect of timber harvesting on soil chemical ingredients and stream water quality”, 「The Korean Journal of Ecology」, 23(1): 9-15.
- Woo, B.-M.(2000), “Brief Introduction on the Forest Hydrological Experiment Station at Choosan”, 「Res Bull. of Seoul National University Forests」, 36: 96-128.
- Åberg, J. & Wallin, M.B.(2014), “Evaluating a fast headspace method for measuring DIC and subsequent calculation of pCO₂ in freshwater systems”, *Inland Waters*, 4(2): 157-166.
- Abril *et al.*(2005), “Carbon dioxide and methane emissions and the carbon budget of a 10-year old tropical reservoir (Petit-Saut. French Guiana)”, *Global biogeochemical cycles*, 19(4).
- Abril *et al.*(2006), “In-Situ measurements of dissolved gases (CO₂ and CH₄) in a wide range of concentrations in a tropical reservoir using an equilibrator”, *Science of the Total Environment*, 354(2): 246–251.
- Abril *et al.*(2014), “Technical Note: Large overestimation of pCO₂ calculated from pH and alkalinity in acidic, organic-rich freshwaters”, *Biogeosciences*, 12(1): 67-78.
- Alin, S. R. *et al.* (2011), “Physical controls on carbon dioxide transfer velocity and evasion in low gradient river systems and implications for regional carbon budgets”, *Journal of Geophysical Research: Biogeosciences*, 116(G1).

- Aufdenkampe, A.K. *et al.*(2011), “Riverine coupling of biogeochemical cycles between land, oceans, and atmosphere”, *Frontiers in Ecology and the Environment*, 9 (1): 53-60.
- Billett, M.F. & Moore, T.R.(2008), “Supersaturation and evasion of CO₂ and CH₄ in surface waters at Mer Bleue peatland, Canada”, *Hydrological Processes*, 22(12): 2044–2054.
- Borges, A.V. *et al.*(2004), “Variability of the gas transfer velocity of CO₂ in a macrotidal estuary (the Scheldt)”, *Estuaries*, 27(4): 593-603.
- Busenberg, E. & Plummer, N. L.(1987), *pH measurement of low-conductivity waters: U. S. Geological Survey Water-Resources Investigation Report 87-4060*.
- Butman, D. & Raymond, P. A.(2011), “Significant efflux of carbon dioxide from streams and rivers in the United States”, *Nature Geoscience*, 4(12): 839–842.
- Cole, J.J., Nina, J. & Caraco, F.(1998), “Atmospheric exchange of carbon dioxide in a low-wind oligotrophic lake measured by the addition of SF₆”, *Limnology and Oceanography*, 43(4): 647-656.
- Cole, J.J. *et al.*(2007), “Plumbing the Global Carbon Cycle: Integrating Inland Waters into the Terrestrial Carbon Budget”, *Ecosystems*, 10(1): 172-185.
- Crawford, J.T. *et al.*(2013), “Emissions of carbon dioxide and methane from a headwater stream network of interior Alaska”, *Journal of Geophysical Research: Biogeosciences*, 118(2): 482-494.
- Davidson, E.A. *et al.*(2010), “Dissolved CO₂ in small catchment streams of eastern Amazonia: A minor pathway of terrestrial carbon loss”, *Journal of Geophysical Research: Biogeosciences*, 115 (G4).
- Dawson, J.J.C. *et al.*(2001), “Is in-stream processing an important control on spatial changes in carbon fluxes in headwater catchments?”, *Science of the Total Environment*, 265(1): 153-167.
- Dinsmore, K.J. *et al.*(2011), “Greenhouse gas losses from peatland pipes: A major pathway for loss to the atmosphere?”, *Journal of Geophysical Research: Biogeosciences*, 116(G3).
- Dinsmore, K.J. *et al.*(2013), “Contrasting CO₂ concentration discharge dynamics in headwater streams: A multicatchment comparison”, *Journal of Geophysical Research: Biogeosciences*, 118(2): 445-461.

- Finlay, J.C.(2003), “Controls of streamwater dissolved inorganic carbon dynamics in a forested watershed”, *Biogeochemistry*, 62(3):231–252.
- Frankignoulle, M. & Borges, A. V. (2001), “Direct and indirect pCO₂ measurements in a wide range of pCO₂ and salinity values”, *Aquatic Geochemistry*, 7(4): 267–273.
- Halbedel, S. & Koschorreck, M. (2013), “Regulation of CO₂ emissions from temperate streams and reservoirs”, *Biogeosciences*, 10: 7539–7551.
- Ho *et al.*(1997), “The effect of rain on air–water gas exchange”, *Tellus B*, 49(2): 149-158.
- Hope, D. *et al.*(1994), “A review of the export of carbon in river water: fluxes and processes”, *Environmental Pollution*, 84(3): 301–324.
- Hope, D. *et al.*(1995), “A method for measuring free CO₂ in upland streamwater using headspace analysis”, *Journal of Hydrology*, 166(1): 1-14.
- Hope, D. *et al.*(2001), “Carbon dioxide and methane evasion from a temperate peatland stream”, *Limnology and Oceanography*, 46(4): 847–857.
- Hunt C.W. *et al.*(2011), “Contribution of non-carbonate anions to total alkalinity and overestimation of pCO₂ in New England and New Brunswick rivers”, *Biogeosciences*, 8(10): 3069-3076.
- Humborg, C. *et al.*(2010), “CO₂ supersaturation along the aquatic conduit in Swedish watersheds as constrained by terrestrial respiration, aquatic respiration and weathering”, *Global Change Biology*, 16(7): 1966–1978.
- IPCC (Eds.) (2007), *Climate Change 2007: The Physical Science Basis. Contribution of Working Group I to the Fourth Assessment Report of the Intergovernmental Panel on Climate Change*, Cambridge and New York: Cambridge University Press.
- Jeong, J.-J. *et al.*(2012), “Differential storm responses of dissolved and particulate organic carbon in a mountainous headwater stream, investigated by high-frequency, in situ optical measurements”, *Journal of Geophysical Research: Biogeosciences*, 117(G3).
- Johnson, M.S. *et al.*(2008), “CO₂ efflux from Amazonian headwater streams represents a significant fate for deep soil respiration”, *Geophysical Research Letters*, 35(17).
- Jones, J.B. & Mulholland, P.J.(1998), “Influence of drainage basin topography and elevation on carbon dioxide and methane supersaturation of stream water”, *Biogeochemistry*, 40(1): 57-72.

- Jonsson, A. *et al.*(2007), “Integrating aquatic carbon fluxes in a boreal catchment carbon budget”, *Journal of Hydrology*, 334(1): 141–150.
- Kim, S. J., Kim, J., & Kim, K.(2010), “Organic carbon efflux from a deciduous forest catchment in Korea”, *Biogeosciences* 7(4): 1323–1334.
- Koprivnjak, J.F., Dillon, P. J., & Molot, L. A.(2010), “Importance of CO₂ evasion from small boreal streams”, *Global Biogeochemical Cycles*, 24(4).
- Lauerwald, R. *et al.*(2013), “What controls the spatial patterns of the riverine carbonate system? — A case study for North America”, *Chemical Geology*, 337: 114–127.
- Li, S.Y. & Zhang, Q.F.(2014), “Partial pressure of CO₂ and CO₂ emission in a monsoon-driven hydroelectric reservoir (Danjiangkou Reservoir), China”, *Ecological Engineering*, 71: 401-414..
- Liss, P. S. & Slater, P. G.(1974), “Flux of gases across the air-sea interface”, *Nature*, 247: 181-184.
- Maria de Fátima, F. L. *et al.*(2013), “Spatial and temporal variability of pCO₂ and CO₂ efflux in seven Amazonian Rivers”, *Biogeochemistry*, 116(1-3): 241–259.
- Millero, F. J.(2000), The carbonate system in marine environments, In A. Gianguzza, & E. Pelizzetti, & S. Sammartano (Eds.), *Chemical Processes in Marine Environments* (pp.9-41), Springer.
- Neal, C. & Thomas, A.G.(1985), “FIELD AND LABORATORY MEASUREMENT OF pH IN LOWCONDUCTIVITY NATURAL WATERS”, *Journal of Hydrology*, 79: 319-322.
- Peter *et al.*(2014), “Scales and drivers of temporal pCO₂ dynamics in an Alpine stream”, *Journal of Geophysical Research: Biogeosciences*, 119(6): 1078-1091.
- Pinol, J. & Avila, A.(1992), “Streamwater pH, alkalinity, pCO₂ and discharge relationships in some forested Mediterranean catchments”, *Journal of Hydrology*, 131(1): 205-225.
- Raymond, P.A., Bauer, J.E., & Cole, J.J.(2000), “Atmospheric CO₂ evasion, dissolved inorganic carbon production, and net heterotrophy in the York River estuary”, *Limnology and Oceanography*, 45(8): 1707-1717.
- Raymond P.A., Caraco, F., & Cole, J.J.(1997), “Carbon Dioxide Concentration and Atmospheric Flux in the Hudson River”, *Estuaries*, 20(2): 381-390.

- Raymond, P.A. & Cole, J.J. (2001), "Gas Exchange in Rivers and Estuaries: Choosing a Gas Transfer Velocity", *Estuaries*, 24(2): 312–317.
- Raymond, P.A. *et al.* (2012), "Scaling the gas transfer velocity and hydraulic geometry in streams and small rivers", *Limnology and Oceanography: Fluids and Environments*, 2(1): 41–53.
- Raymond, P.A. *et al.* (2013), "Global carbon dioxide emissions from inland Waters", *Nature*, 503(7476): 355-359.
- Sarmiento, J. L. & Gruber, N. (2006), *Ocean Biogeochemical Dynamics*, Princeton: Princeton University Press.
- Schlesinger, W. H. & Bernhardt, E.S. (2013), *Biogeochemistry: an analysis of global change*, San Diego: Academic press.
- Schwarzenbach, R.P., Gschwend, P.M., & Imboden, D.M. (2003), *Environmental organic chemistry, 2nd eds.*, Hoboken: Wiley Interscience.
- Shin, W.J. *et al.* (2011), "Dissolved inorganic carbon export from carbonate and silicate catchments estimated from carbonate chemistry and $\delta^{13}\text{C}$ DIC", *Hydrology and Earth System Sciences*, 15(8): 2551-2560.
- Siegenthaler, U. & Sarmiento, J.L. (1993), "Atmospheric carbon dioxide and the ocean", *Nature*, 365(6442): 119-125.
- Stumm, W. & Morgan, J.J. (1996), Dissolved carbon dioxide, In W. Stumm & J.J. Morgan (Eds.), *Aquatic Chemistry* (pp.148-205), Wiley-Interscience.
- Teodoru, C.R. *et al.* (2009), "Patterns in pCO₂ in boreal streams and rivers of northern Quebec, Canada", *Global Biogeochemical Cycles*, 23(2).
- Wallin, M.B. *et al.* (2011), "Spatiotemporal variability of the gas transfer coefficient (K_{CO_2}) in boreal streams: Implications for large scale estimates of CO₂ evasion", *Global Biogeochemical Cycles*, 25(3).
- Wallin, M.B. *et al.* (2012), "Evasion of CO₂ from streams – The dominant component of the carbon export through the aquatic conduit in a boreal landscape", *Global Change Biology*, 19(3): 785-797.
- Wallin, M.B. *et al.* (2013), "Evasion of CO₂ from streams - The dominant component of the carbon export through the aquatic conduit in a boreal landscape", *Global Change Biology*, 19(3): 785-797.

- Wanninkhof, R.(1992), “Relationship between wind speed and gas exchange over the ocean”, *Journal of Geophysical Research: Oceans (1978–2012)*, 97(C5): 7373-7382.
- Weiss, R.R.(1974), “Carbon dioxide in water and seawater: the solubility of a non-ideal gas”, *Marine chemistry*, 2(3): 203-215.
- Wetzel, R.G.(1983), *Limnology, 2nd edn.*, Philadelphia: Saunders College Publishing.
- Wetzel, R.G. & Likens, G.E.(1991), *Limnological Analysis, 2nd edn.*, New York: Springer-Verlag.
- Whitman, W. G.(1923), “The two-film theory of gas absorption”, *Chemical and Metallurgical Engineering*, 29(146).
- Zappa, C.J. *et al.*(2003), “Variation in Surface Turbulence and the Gas Transfer Velocity over a Tidal Cycle in a Macro-tidal Estuary”, *Estuaries*, 26(6): 1401–1415.
- Zeng, F.W. & Masiello, C.A.(2010), “Sources of CO₂ evasion from two subtropical rivers in North America”, *Biogeochemistry*, 100(1-3): 211–225
- Alin, S.R. *et al.*(2005), carbon dioxide Evasion from Large Tropical Rivers: Measurements from the Amazon and Mekong River Basins, <http://www.co2.ulg.ac.be/objects/2005/ppt/alin.pdf>.
- Korea Meteorological Administration, <http://www.kma.go.kr/>.
- Korea Institute of Geoscience and Mineral Resources, Geological resources information system, <http://geoinfo.kigam.re.kr>.
- Lewis and Wallace (1998), Program Developed for CO₂ System Calculations. ORNL/CDIAC-105. Carbon Dioxide Information Analysis Center, Oak Ridge National Laboratory, U.S. Department of Energy, Oak Ridge, Tennessee.
- NOAA, Carbon Dioxide at NOAA’s Mauna Loa Observatory reaches new milestone: Tops 400 ppm, <http://www.esrl.noaa.gov/news/2013/CO2400.html>.
- The Global Carbon Project, Global carbon budget, www.globalcarbonproject.org.

국문초록

하천에서 대기 중으로 직접 배출되는 이산화탄소의 양은 지역적 또는 전 지구적 탄소수지에서 중요한 항목임에도 불구하고 이에 대한 연구는 많이 진행되지 않았다. 이는 육상수계에서 하천이 차지하는 면적이 상대적으로 적고, 수체로부터의 이산화탄소 가스수송속도를 추정하는 것과 강우 시 시시각각 바뀌는, 하천의 폭과 깊이와 같은 하천의 지형학적 정보를 얻기 어렵기 때문이다. 이 연구는 전라남도 광양시 백운산 내 서울대학교 남부학술림 북문골 유역을 대상으로 산림유역의 계류수로부터 대기 중으로 직접 배출되는 이산화탄소의 연간 배출량을 정량하였다. 이를 위해 2012 년 5 월부터 2014 년 4 월까지 매주, 또한 여름철 집중 강우 시 2-4 시간 간격으로 채취된 북문골 계류수를 사용하였다. 이 연구의 목적은 첫째, 산림유역 계류수를 대상으로 연간 대기 중으로 배출되는 이산화탄소를 정량 하여, 하천을 통해 유출되는 연간 용존무기탄소의 양과 비교하고, 둘째, 이에 영향을 끼치는 요소들이 무엇인지 조사하는 것이다. 계류수의 pH, 수온, 알칼리도를 이용하여 하천 내 이산화탄소와 평형 상태에 있는 대기 중 이산화탄소의 분압을 계산하였다. 이와 함께, 가스수송속도를 추정하기 위하여 하천에 적합한 3 개의 경험식을 사용하여 계류수로부터 방출되는 이산화탄소의 양을 추정하였다. 그 결과 백운산 산림유역 계류수에서 대기 중으로 배출되는 연간 유역 면적당 이산화탄소의 양은 $0.06 - 0.12 \text{ g C m}^{-2} \text{ yr}^{-1}$ 으로 추정되었으며, 이는 하천을 통해 유출되는 연간

용존무기탄소 양의 최대 약 12%에 해당한다. 특히, 여름철 호우기에 비가 집중적으로 내림에 따라 유량이 증가하고 함께 늘어난 유속으로 인해 가스수송속도가 증가하며, 따라서 산림유역 계류수 내 이산화탄소가 대기 중으로 더 많이 유출될 수 있다. 세가지 경험식으로부터 계산된 가스수송속도는 2.3 m d^{-1} 에서 115 m d^{-1} 으로 범위를 보였고, 따라서 매주 채취된 시료로부터 계산된 계류수로부터의 이산화탄소 배출량의 변이 폭이 커질 수 있다. 비록 산림 유역에서 계류수가 차지하는 면적은 적지만, 이 연구 결과는 계절풍 기후대 내 온대산림 계류수로부터 대기로 이동하는 이산화탄소의 양이 지역 내 탄소 순환의 중요한 요소임을 의미한다.

주요어 : 가스수송속도, 산림, 유역, 계절풍 기후, 이산화탄소 분압, 하천

학 번 : 2012-23783